Effect of moisture content on hygrothermal properties: Comparison between pith and hemp shiv composites and other construction materials

Mohamed Said Abbas, Fionn Mcgregor, Antonin Fabbri, Mohammed Yacine Ferroukhi, Céline Perlot-Bascoules

Version of Record: https://www.sciencedirect.com/science/article/pii/S0950061822014064
Manuscript_60c5f4d63197a12e21c74fe5c0eecc69

Effect of moisture content on hygrothermal properties: comparison between pith and hemp shiv composites and other construction materials

Mohamed Said ABBAS[a*], Fionn McGREGOR[a], Antonin FABBRI[b], Mohammed Yacine FERROUKHI[c], Céline PERLOT[a]

[a] Université de Pau et des Pays de l'Adour, E2S UPPA, SIAME, Anglet, France
[b] Univ Lyon, ENTPE, LTDS UMR CNRS 5513, Vaulx-en-Velin Cedex, F-69518, France
[c] Univ Lyon, ENISE, LTDS UMR CNRS 5513, St-Etienne Cedex, F-42023, France
[*]Corresponding author; e-mail: mohamed-said.abbas@univ-pau.fr

Abstract
This paper deals with the experimental assessment of the influence of water content on thermal conductivity, thermal effusivity, heat capacity and vapor permeability of pith and hemp shiv composites. The results, which will be used to enrich modelling databases, show that all four properties increase their value with relative humidity, especially for pith composites, while remaining within adequate margins. They are compared to the results commonly measured for other porous construction materials, namely hemp concrete, wood, and rammed earth. This comparison allows to better understand the influence of the material morphology and nature on hygrothermal properties in presence of moisture. It has been noted that, in hygroscopic conditions, the specific heat cannot always be deduced from the specific heat of water and of the dry material due to the interactions between the adsorbed water and the material. On the other hand, the transport of liquid water has been observed to play a significant role in the hygroscopic transfers.

Keywords: Bio-based materials, hygrothermal properties, hemp shiv, sunflower and maize pith, rammed earth, moisture

1. Introduction

Bio-based composites are very promising to reduce the carbon footprint of buildings as they can be locally sourced from agricultural by-products (Amziane et al., 2017; Amziane & Sonebi, 2016). They also have strong hygrothermal properties (A. Fabbri & McGregor, 2017; Palumbo et al., 2016) while being highly hygroscopic, which means that water vapor can go through them and that they can store it.

Hygrothermal properties are at the heart of numerous studies that seek to develop eco-friendly construction materials (Cagnon et al., 2014; Liuzzi et al., 2018; Vololonirina et al., 2014), since such properties still remain a challenge when considering them in the calculation of building energy efficiency. Highly hygroscopic materials have the potential to reduce the energy consumption used for heating and cooling of the building (Allinson & Hall, 2010), which represent approximately 40% of the energy consumption in buildings according to (International Energy Agency & UN Environment Programme, 2019). Buildings' operation, for its part, is to blame for 35% of the global energy consumption according to (International Energy Agency & UN Environment Programme, 2020).

In this paper, four hygrothermal parameters will be addressed: the thermal conductivity, the thermal effusivity, the heat capacity and the water vapor permeability. Thermal conductivity (λ) is one key hygrothermal property which indicates whether a material is a good heat conductor or not. Insulating materials have repeatedly proven to significantly reduce thermal loss and, therefore, energy consumption (Al-Homoud, 2005; Cholewa et al., 2020; Grillone et al., 2020; Lu & Warsinger, 2020; Sadineni et al., 2011). Thermal effusivity (e), on its side, denotes a material's ability to exchange thermal energy with its surroundings. According to (Shrotriya et al., 1991), it describes the transient heat accumulation capacity of materials due to a change in the temperature of the ambient, which leads to a change of the material's surface temperature. Hence, a material with low thermal effusivity will heat fast in its surface with a low heat intake and will give a sensation of warmth to touch. Heat

capacity (C_p) represents the material's capacity to store heat, which is strongly related to thermal mass or thermal inertia, typically offered by dense materials since the specific heat of a material depends on its density (Howlader et al., 2012). Materials with high heat capacity contribute to the temperature stability of the building. Lastly, water vapor permeability (δ_p), which stands for the ability to let water vapor pass through, has a great influence on heat loss because of coupled heat and moisture transfers.

Since all material properties in eco-friendly and hygroscopic building materials, such as thermal conductivity, thermal effusivity, heat capacity and water vapor permeability, have been reported to be influenced by the water content which varies with indoor humidity levels (Houngan et al., 2015; Rahim et al., 2016; Seng et al., 2017), it is important to ensure that these properties remain in an acceptable range for all plausible humidity conditions.

The value of all the aforementioned properties globally increases with water content, but the way it does can capitally change from one material to another.

(Kočí et al., 2017) considered three types of load-bearing materials (autoclaved aerated concrete, high performance concrete and solid clay brick) and found that thermal conductivity increases with the water content in different ways depending on the pore structure and the solid matrix properties. For high performance concrete, the correlation described an exponential, whereas it was linear for autoclaved aerated concrete and parabolic for clay brick. Solid clay brick tripled its dry thermal conductivity at 25% volumetric water content, while for autoclaved concrete it was multiplied by 8 while staying low. They also studied the evolution of specific heat with equally disparate results. Much like Kočí, (Meukam et al., 2004) studied several building materials made up of lateritic soil and cement and found an irregular increase of thermal conductivity with water content, different for each material.

(Real et al., 2016) studied the thermal conductivity of different composites made of expanded clay, fly ash and expanded slate with a common binder, CEM I. They found that, for a common water/binder ratio, the evolution of their thermal conductivity normalized to the dry thermal conductivity with water content followed a common linear relation for all composites. (Toman & Černý, 2001) represented the variation of specific heat with water content for Temelin and Penly, two high performance concretes, and found a linear relation with similar slopes for both materials. In the same direction, (Tran Le, 2010) noted that thermal conductivity and water content are related by a linear tendency for several kinds of concrete, including hemp concrete. This last had the lowest slope and appeared to have low thermal effusivity.

Bio-based composites have also been subject to several studies relating material properties and water content. (Boukhattem et al., 2017) noted an exponential tendency between the thermal conductivity of date palm fiber composites and their water content, as did (Taoukil et al., 2013) for wood composites and (Belkharchouche & Chaker, 2016) for olive pomace composites. As for the thermal effusivity of bio-based materials, (Houngan et al., 2015) studied the dependence between the water content and the tangential thermal effusivity for two types of wood and found an almost linear increase with very similar slopes for both kinds of wood. (Bouguerra, Diop, et al., 1998) reached the same result for wood cement-based composites, observing an almost constant positive slope between both magnitudes.

Hemp composites are perhaps the most documented bio-based composites and there is no exception when it comes to the influence of water content on hygrothermal properties. (Collet & Pretot, 2014) found that the thermal conductivity of different hemp composites increases linearly with water content. (Gourlay et al., 2017) and (Bennai et al., 2018) found very similar tendencies for thermal conductivity, but heat capacity was more controversial. While (Bennai et al., 2018) reported a

significant increase of the heat capacity with water content for hemp shiv concrete, (Gourlay et al., 2017) found an almost linear increase between specific heat capacity and water content for defibrated hemp straw formulations but an almost constant specific heat capacity for formulations with fibred hemp shiv. (De Bruijn & Johansson, 2013) observed a milder increase for both the thermal conductivity and heat capacity of a lime-hemp concrete. The study of the C_p of hemp composites has been addressed as well by (Walker & Pavía, 2014), who found that the type of binder does not have a clear impact on the heat capacity, but that there exists a trend that suggests that the binder hydraulicity yields higher C_p values and lower thermal conductivities. On the other hand, (Gourlay et al., 2017) noted that the nature of the hemp shiv does have a significant impact on the specific heat capacity.

Water vapor permeability has been noted to change when measured at different relative humidity pairs (%RH in and outside the cup) by several authors. (Latif et al., 2014) compared the vapor diffusion resistance factor obtained at 0/50%RH and at 50/93%RH for a hemp-lime wall, a plasterboard and two wood wool boards and, in every case, the results for different humidity conditions deferred substantially, 0/50%RH results being greater than the results for 50/93%RH. This means that water vapor goes through the material more easily when relative humidity is high. (Colinart et al., 2013) found rather disparate values for a hemp concrete wall when the test was carried at 0/50%RH and at 50/85%RH, as did (Bennai et al., 2018) for 3/50%RH and 93/50%RH. In all cases, moisture transfer seems to involve both vapor and liquid transport, and lower humidity conditions yield lower permeability values. (Ouméziane et al., 2012) performed tests on a hemp concrete wall at different humidity pairs and found that water vapor permeability increases with water content, describing a power law.

Regarding pith composites, there is very little available information. (Brouard et al., 2017) and (Brouard et al., 2018) focused on the study of clay-sunflower and rape straw composites. They found the thermal conductivity to increase with water content describing a non-linear tendency similar to the one found by (J. P. Laurent & Guerre-Chaley, 1995) at 20-30°C.

Maize and sunflower pith composites are materials with very promising thermal and hygroscopic properties (Abbas et al., 2020, 2019), as well as acoustic characteristics (Abbas, Fabbri, et al., 2021; Abbas, Gourdon, et al., 2021), made out of a very light agricultural by-product that has a particularly low thermal conductivity (Pennec et al., 2013) at low water content. In France, pith constitutes a more accessible alternative to hemp shiv, since maize and sunflower culture is more widespread than hemp's, with 1.57 Mha and 690 000 ha cultivated each year in the country, respectively, against only 15 000 ha for hemp (Arvalis, 2020; Guyomard, 2020; InterChanvre, 2018). Unfortunately, a lack of information about these materials has been noted, especially regarding the evolution of their behavior with humidity, information that is necessary namely for reliable hygrothermal simulations, which are powerful tools for assessing the benefits of the use of bio-based materials on the energy consumption and on the hygric comfort in buildings.

This paper focuses on the study of sunflower pith-lime composites, maize pith-lime composites, and hemp shiv-lime composites, as well as the analysis of the impact of water content on the aforementioned hygrothermal properties, comparing them to other building materials studied in literature. Thermal conductivity and thermal effusivity will be measured using a hot wire and a hot plan device, respectively, while water vapor permeability will be assessed through wet cup and dry cup measurements. The different water contents will be obtained by placing samples in atmospheres in which the relative humidity is controlled with saline solutions, with salt or with silica gel.

2. Materials and methods

2.1. Materials

2.1.1. Plant aggregates

Three types of vegetal aggregates were used in this study, which are shown in **Figure 1**. The first one is denoted as S and is a sunflower pith with a 14 kg/m^3 bulk loose density and an average diameter of about 2 mm. The second, denominated M, is a maize pith with a bulk loose density of 18 kg/m^3 and an average diameter of about 4 mm. The third type of aggregate is hemp shiv, denoted as H, whose loose density is about 100 kg/m^3 and whose average length and width are about 8 and 4 mm, respectively. The dimensions of the different aggregates were measured by image analysis and through sieve analysis. The image analysis allows to deduce the length and width of a group of aggregates spread on a surface by taking a picture and by measuring them with a dedicated software. The sieve analysis is more adapted to spherical aggregates, and it is used to measure the diameter by sieving the aggregates with different sieve opening sizes and by measuring the number of particles that are retained in each sieve.

Figure 1 Sunflower pith (left), maize pith (middle) and hemp shiv (right).

2.1.2. Binders

Three binders have been used throughout this experimental campaign. The first is called HB and it is a cement and lime mixture with further additives, whose exact composition is not available for it was developed by an industrial partner. The second is called C1 and is a calcic-lime-based binder, while the third binder is called C2 and is made up of hydraulic lime, calcareous charges, hydrophobic and rheological admixtures.

2.1.3. Formulations and manufacturing

The different composites manufactured from the three aggregates and the three binders are detailed in **Table 1**, along with their exact formulation and the dry density of each formulation. Some of them are shown in **Figure 2**.

Table 1 Summary of the formulation, mass ratio and dry density of the composites.

Type of binder	**HB**		**C1**	**C2**		
Type of aggregate	S	M	H	H*	S	H+S
Designation	HB-S	HB-M	C1-H	C2-H*	C2-S	C2-H+S
Hemp shiv/ binder [-]**	0	0	0.33	0.33	0	0.17
Pith/binder [-]**	0.20	0.16	0	0	0.10	0.06

Water/binder [-]**	2.92	2.92	0.81	0.88	0.80	1.07
Mass proportion of hemp shiv [-]	0	0	0.15	0.15	0	0.07
Mass proportion of pith [-]	0.05	0.04	0	0	0.05	0.03
Dry density [kg/m^3]	150 ± 4	160 ± 5	470 ± 5	600 ± 10	550 ± 5	590 ± 6

* corresponds to a formulation which has been densified using a tamper tool

** correspond to mass ratio between constituents

All samples were sprayed in 16 cm diameter and 32 cm high cylindrical formworks and compacted at 0.05 MPa according to (Association construire en chanvre & Fédération Française du Bâtiment, 2009). They were all manufactured at 50%RH and 23°C in a single layer, except for C2-H*, which was manufactured in 6 layers of 5 cm each and compacted layer by layer. The asterisk in C2-H* means that it has been densified using a tamper tool. The samples used in the thermal tests (conductivity, effusivity and specific heat) were core drilled and sawed into 10 cm diameter, 4 cm high cylinders. For the permeability test, the resulting samples were 10 cm diameter cylinders with three different thicknesses: 2, 4 and 6 cm.

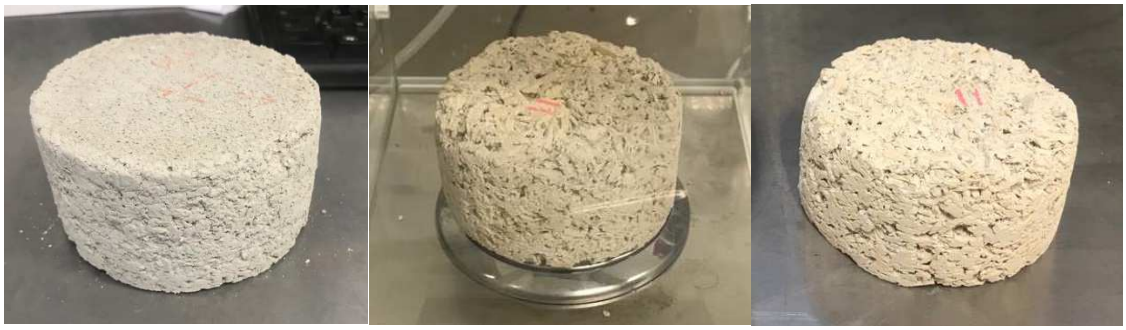

Figure 2 HB-S (left), C1-H (middle) and C2-H+S samples.

Samples were tested 6 months after manufacturing, period during which they were stored in a room at 23°C (±5°C) and 50%RH (±5%RH). Right before testing, samples were oven-dried at 50°C and at relative humidity levels lower than 5%RH until stabilization to start all tests at the dry state, and their mass was measured. We consider that the sample has stabilized if the mass variation between two measures performed with a 24-hour difference is under 0.01%, which can take several days.

2.2. Methods

2.2.1. Variation of the thermal conductivity and thermal effusivity with water content

The thermal conductivity, denoted λ and expressed in [mW/(m.K)], of HB-S, C2-H*, C2-H+S, C2-S and C1-H at different water content values was measured using the well-known hot wire method. The FP2C device was used following ISO 8894-2 standard (International Organization for Standardization, 2007). The thermal effusivity (e) of the same materials is measured using the hot plan method, which is performed using the same FP2C apparatus with a hot plan probe. It is expressed in [J/(m^2.K.s$^{1/2}$)]. A constant heat flux is imposed by positioning the thin flat heating plate between two superposed cylindrical samples.

In order to reach different water content levels, conditioned samples were placed inside ventilated boxes, one box for each relative humidity target value. Each value is reached by using a different saline solution. Two samples of each formulation are placed in each box until they stabilize, which can take several weeks. The elevated duration of the test is the reason why different humidity conditionings are conducted in parallel and therefore, an important number of samples is needed.

Once the water content of the samples placed inside each box has stabilized (meaning that the mass variation in 24 hours is under 0.1%), the FP2C is introduced inside the box and both thermal conductivity and thermal effusivity are measured three times for each two samples by placing the probe between them. The ambient temperature is 23 ±1°C. The mass water content (u) is calculated as the difference between the stabilized wet mass (m_{wet}) and the dry mass (m_{dry}) of each sample, divided by the dry mass, as shown in **Equation 1**.

$$u = \frac{m_{wet} - m_{dry}}{m_{dry}} \qquad (1)$$

The given thermal conductivity and effusivity results are the arithmetic average of the three weighings.

2.2.2. Specific heat capacity

The specific heat capacity (C_p) is determined from the measurements of the thermal conductivity and thermal effusivity previously detailed, since the three properties are linked through the definition of the thermal effusivity:

$$e = \sqrt{\lambda \rho C_p} \qquad (2)$$

Where e is the thermal effusivity expressed in [J/(m^2.K.s$^{1/2}$)], λ is the thermal conductivity expressed in [W/(m.K)], ρ is the density of the material in kg/m^3 and C_p is the specific heat capacity in [J/(kg.K)]. The product ρC_p represents the volumetric heat capacity in [J/(m^3.K)].

2.2.3. Water vapor permeability

The dry cup and wet cup methods were used to determine the vapor permeability of C2-H*, C2-H+S, C2-S, HB-S and HB-M samples. The permeability of C1-H could not be determined because the material belongs to a previous experimental campaign and not enough samples were left. Both tests were conducted following the standard EN ISO-12572 (International Organization for Standardization, 2016). Samples were placed in cups, sealed to the cup with silicone and scotched with aluminum foil following (McGregor et al., 2014)'s indications.

Table 2 Summary of the tested humidity pairs for each formulation.

	HB-S	HB-M	C2-H*	C2-H+S	C2-S
Dry cup	3/23%RH	3/23%RH	3/54%RH	3/54%RH	3/54%RH
	23/63%RH	63/85%RH	23/71%RH	23/71%RH	23/71%RH
	33/68%RH	75/85%RH	-	-	-
Wet cup	93/23%RH	63/33%RH	85/54%RH	85/54%RH	85/54%RH
	75/63%RH	75/63%RH	85/71%RH	85/71%RH	85/71%RH
	85/63%RH	-	-	-	-

Several relative humidity pairs, identified in **Table 2**, were tested for each sample using saline solutions, salt only or silica gel, in the case of 3%RH. The first relative humidity value in each cell can be calculated from P_v^{cup} ($RH = \frac{P_v}{P_{v,sat}}$), which is pictured in **Figure 4**, and the second one can be deduced from

$P_v^{exterior}$ through the same formula. For the dry cups, water-free salt was added to the inside of the cup to maintain a minimum thickness of the air layer, which measures 3 cm at the beginning of the test (see **Figures 3 and 4**). Three samples of thickness 2, 4 and 6 cm of each formulation were tested for each relative humidity pair, in order to apply the so-called β-correction, which stands for the global film resistance correction, and which can be calculated following **(3)** and **(4)**:

$$\frac{G}{S} = \delta_a \frac{P_v^{cup} - P_v^{surface\,1}}{da} \quad (3)$$

$$\frac{G}{S} = \beta\left(P_v^{surface\,2} - P_v^{exterior}\right) \quad (4)$$

Where G is the total humidity flow in [kg/s], S is the sample's surface in [m²], δ_a is the water vapor permeability of air in [kg/(m·s·Pa)], da is the thickness of the air layer in [m], β is the coefficient of surface water vapor transfer in [kg/(m²·s·Pa)] (McGregor et al., 2017) and P_v^{cup}, $P_v^{surface\,1}$, $P_v^{surface\,2}$ and $P_v^{exterior}$ are the vapor pressures represented in **Figure 4**.

The tests were carried out in a single ventilated glove box with a temperature of 23 ± 0.5°C. The ventilation of the box ensured that the air velocity over each sample was at least 2.2 m/s. Each sample-cup assembly was weighed every 24 hours to monitor the mass transfer. The mass of the wet cup assemblies decreased whereas the mass of the dry cup assemblies increased. After an initial stabilization period, a constant mass flow rate is achieved, which means that a linear function correlates the mass variation with time. The humidity and temperature inside the cups and inside the glove box were continuously monitored during the test to ensure that they remained constant. When the test is complete, the samples are weighed without the cup, silicone and aluminum tape to determine their water content, and then dried at 50°C and relative humidity values lower than 5%RH in an oven until the mass is stabilized, after which their dry mass is measured.

Figure 3 Dry cups with silica gel (left) and wet cups with saline solution (right).

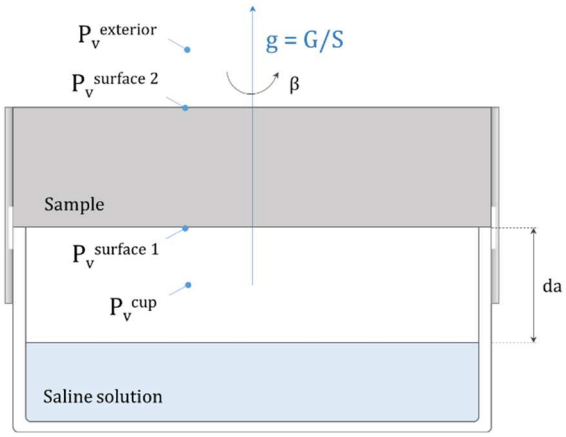

Figure 4 Illustration of a wet cup.

3. Results

3.1. Impact of moisture content on thermal conductivity

The impact of the moisture content on the thermal conductivity of the composites HB-S, C2-H*, C2-H+S, C2-S and C1-H has been assessed. As it is shown in **Figure 5**, the increasing moisture content (expressed as saturation rate) causes an increase on the thermal conductivity of the composites, which is coherent since the air within the pores of the material is progressively substituted by water in gaseous or liquid state. The saturation rate (or degree of saturation), denoted Sr, is defined as the ratio between water volume (V_w) and pore volume (V_{pores}). For a non-deformable medium, it can be related to mass (u) and volume (θ) water contents as follows:

$$Sr = \frac{V_w}{V_{pores}} = \phi\theta = \frac{\rho_{dry}}{\rho_w}\phi\, u = \frac{\phi w}{\rho_w} \qquad (5)$$

With ϕ [-] the total open porosity, ρ_{dry} [kg/m^3] and ρ_w [kg/m^3] the density of the dry composite and of water, respectively.

As explained by (Brouard et al., 2017), water vapor forms menisci in the pores above a certain relative humidity threshold, generating thermal bridges. Liquid water has a thermal conductivity about 25 times greater than air's at ambient temperature, whereas water vapor has a thermal conductivity equivalent to air's at 2°C according to (Bouguerra, 1999), but this value becomes 20 times greater at 60°C.

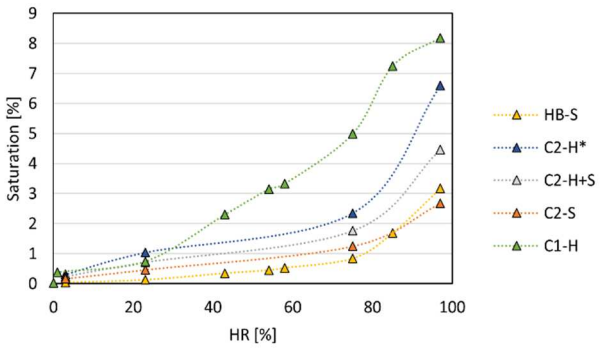

Figure 5 Evolution of the saturation with relative humidity found during thermal conductivity and thermal effusivity tests.

For the maximum relative humidity (97%RH), hemp composites contain more water than pith composites (see **Fig. 5**), which is consistent with the results found in (Abbas et al., 2020). Concerning their thermal behavior, HB-S and C2-S present the lowest values of λ at dry state (see **Fig. 4** left) and, although the difference between the composites containing the binder C2 is barely discernible at low saturation rate, the evolution of the thermal conductivity is very dissimilar. In **Fig. 4** right, the evolution of λ/λ_{dry} with the saturation rate is represented in order to study how the insulating properties of materials are affected as water progressively fills their pores. It can be noted from this figure that the evolution of λ/λ_{dry} is practically linear for all composites and that the increase is more acute for pith composites, especially for C2-S, and less acute for hemp composites, with C2-H+S between both groups.

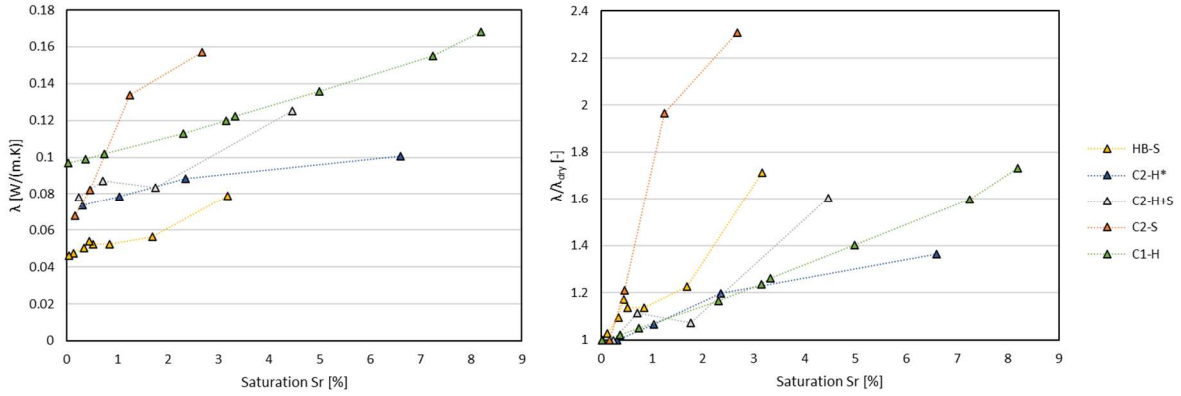

Figure 6 Evolution of thermal conductivity (left) and of thermal conductivity normalized to the dry thermal conductivity (right) with saturation rate of HB-S, C2-H*, C2-H+S, C2-S and C1-H.

3.2. Impact of moisture content on thermal effusivity

As it has been mentioned previously, this parameter is responsible for metal being colder to touch (high thermal effusivity) than, for example, cotton (low thermal effusivity). Regarding building materials that are meant for the inside of the building, a low thermal effusivity is desirable for the sake of thermal comfort.

The dry thermal effusivity of a composite material (a porous material is considered a composite made of a solid phase and air) depends, on the one hand, on the thermal properties of the constituents and, on the other hand, it depends on the distribution of these constituents – their volumetric fraction, their connectivity, etc. (Bouguerra, Ledhem, et al., 1998; Lei et al., 2019).

Figure 7 depicts the evolution of the thermal effusivity of HB-S, C2-H*, C2-H+S, C2-S and C1-H and of the thermal effusivity normalized to the dry value. At the dry state, HB-S presents the lowest effusivity and C1-H the highest, whereas the composites that contain C2 are between both, which suggests that the type of binder has a remarkable influence. The effusivity of the five composites grows with moisture content, as expected (Antczak et al., 2003), since the thermal effusivity of water is about 270 times greater than air's (Bouguerra, Diop, et al., 1998). As explained by Bouguerra et al., the effusivity depends on the ease with which heat is transmitted through the porous material. Consequently, the constrictivity – which is the reduction of the section of the path through which the heat flows – and the tortuosity of the heat paths result in a low effusivity. In the dry state, heat flows mostly through the solid matrix but, in presence of water, heat can flow through both phases. Even at low moisture content, water forms a film on the pores' surface, widening the section of the eventual paths of the heat flux lines, which could only travel through the solid skeleton in the absence of moisture. Moreover, when the moisture content exceeds a certain threshold, the liquid phase inside the material is

considered to be continuous and the tortuosity of the heat flux lines starts to decrease. In both cases, the phenomena result in an increase of the thermal effusivity.

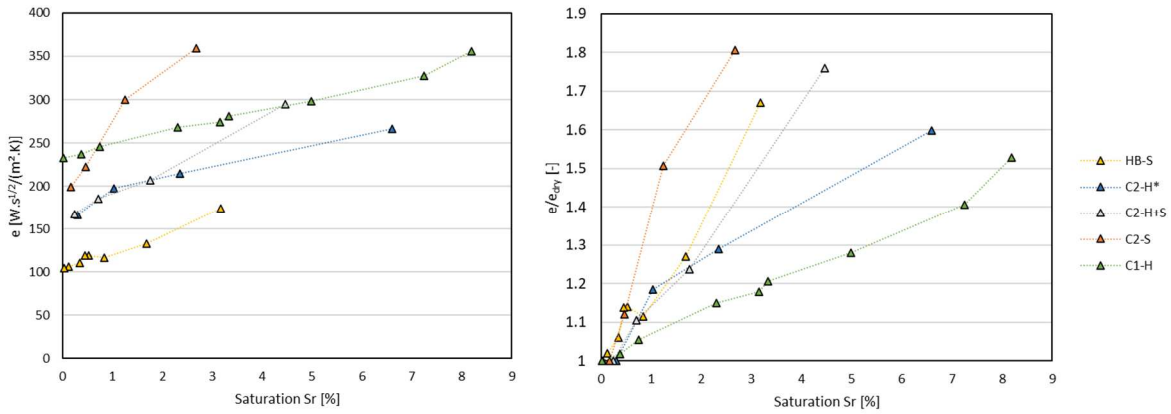

Figure 7 Evolution of the thermal effusivity with saturation rate (left) and of thermal effusivity normalized to the value at dry state (right) of HB-S, C2-H*, C2-H+S, C2-S and C1-H.

For all five composites, the increase of the thermal effusivity is almost linear. The slope of the normalized values is grater for the composites containing pith and lower for hemp composites, very similarly to the behavior described for thermal conductivity.

3.3. Impact of moisture content on specific heat capacity

The evolution of the specific heat capacity C_p of the composites with mass moisture content is pictured in **Figure 8**. At the dry state, HB-S presents the highest value (which is also true for all the moisture range), followed by C1-H, C2-S, C2-H* and C2-H+S.

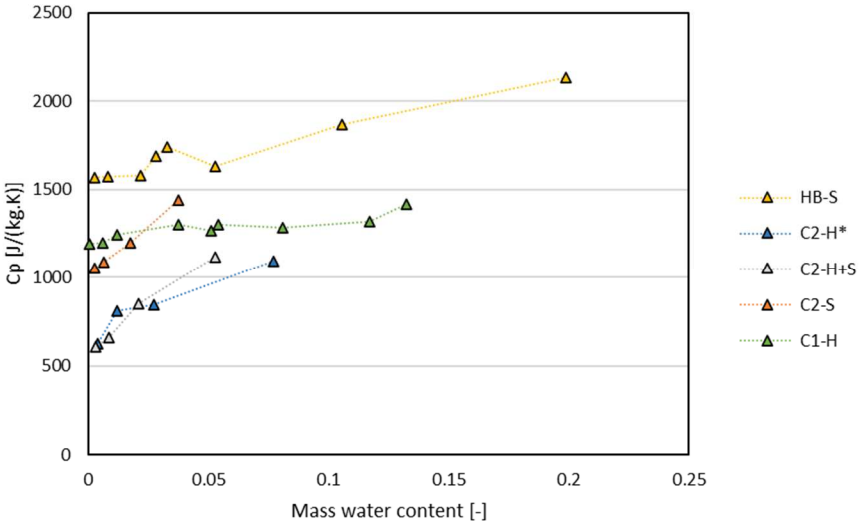

Figure 8 Evolution of the specific heat capacity with the mass moisture content of HB-S, C2-H*, C2-H+S, C2-S and C1-H.

For all composites, the specific heat capacity increases with the presence of moisture, which is consistent with the fact that water gradually replaces air. Whereas the contribution of air is negligible

due to its very low density, the contribution of water is not, and so the total heat capacity increases with water content. The trend for all materials is almost linear.

3.4. Water vapor permeability

The vapor permeability δ_p results at different saturation levels for C2-H*, C2-H+S, C2-S, HB-S and HB-M are shown in **Figure 9**.

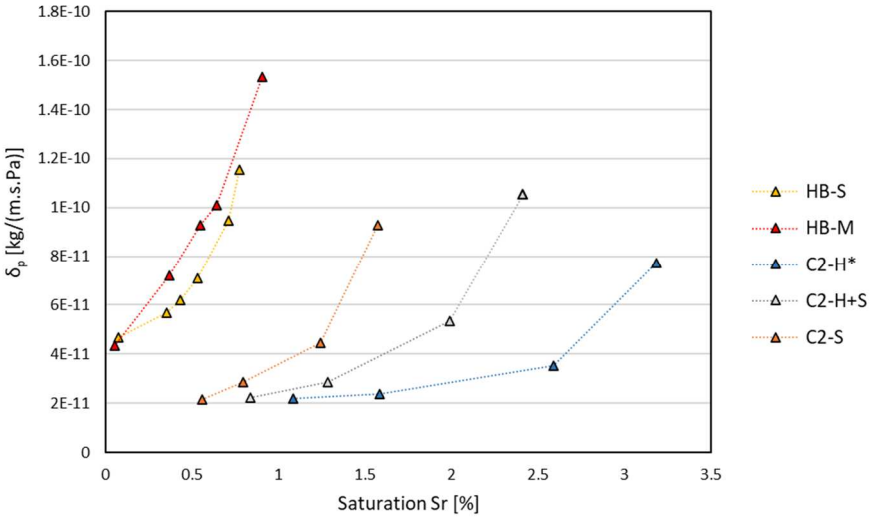

Figure 9 Evolution of water vapor permeability with saturation rate.

For all formulations, the vapor permeability increases with the saturation rate. The binder seems to strongly influence the permeability - saturation trend, since two groups of curves can be distinguished: a first one, consisting of HB-M and HB-S, with a low moisture permeability around 4.5x10^{-11} kg/(m.s.Pa) (which corresponds to a vapor resistance value of $\mu = 4{,}3$) and an increase of about 300% for maximum saturation values; then a second group consisting of C2-S, C2-H+S and C2-H*, with a minimum permeability of about 2.2x10^{-11} kg/(m.s.Pa) (which corresponds to $\mu = 8{,}9$) and an increase of about 400%.

4. Discussion

While some materials are tested for the whole range of moisture content, from the dry material to saturation, the composites studied in this experimental campaign have only been tested for the moisture content range that can be induced by ambient relative humidity (0-97%RH), which is much more limited. The reason of this premise is that these materials are intended to be sheltered from water and, therefore, no source of humidity other than the air moisture will affect them.

4.1. Impact of moisture content on thermal conductivity

While many authors report that the thermal conductivity increases linearly with moisture content for several construction materials (Collet & Pretot, 2014; Gourlay et al., 2017; Hall & Allinson, 2009; Real et al., 2016; Troppová et al., 2015; Yu et al., 2011), others have found an exponential correlation (Belkharchouche & Chaker, 2016; Boutin, 1996; Taoukil et al., 2013). However, the temperature plays a major role in the shape of the curve and must be taken into account, as must be the range of moisture considered (for instance, it cannot be concluded that the correlation is linear or exponential by looking exclusively at the low-moisture content range).

Some papers provide very complete information about these factors and study the thermal conductivity in the whole moisture content range (from the dry material to 100% saturation) and assess the impact of temperature. Some examples are (J. P. Laurent & Guerre-Chaley, 1995), in which the thermal behavior of autoclaved cellular concrete is examined, and (Bouguerra, 1999), which addresses clay-cement wood composites. Both papers explain that, for temperatures under 20 °C, the thermal conductivity increases nearly linearly with the degree of saturation and that, over this temperature, the relationship becomes more curvilinear. The difference lies on the evaporation and condensation phenomena of water, the most important increase of the thermal conductivity happening at a degree of saturation between 0 and 50% for (Bouguerra, 1999) and between 20 and 40% for (J. P. Laurent & Guerre-Chaley, 1995). The low-moisture section of the curvilinear graphs can indeed be interpreted as an exponential function, but the complete high-temperature graphs present more of an "S" shape.

By comparing these results to other authors', it can be noticed that all materials seem to present these two behaviors for the relationship between thermal conductivity and moisture content – a linear growth at low temperature and "S" shaped relationship at higher temperatures – but the temperature threshold is different for each material. Water, whether it is in the liquid or in the gaseous state, presents a higher thermal conductivity at higher temperatures. In addition, at higher temperatures, the interactions between water, air, and matrix change, which could induce a different phase distribution morphology as a function of temperature. These two phenomena favor higher thermal conductivity values of the wet material at high temperatures. Non-linearities for temperatures above ambient temperature (T > 20°C) are, according to (Bouguerra, 1999) and (J. P. Laurent & Guerre-Chaley, 1995), caused by evaporation-condensation phenomena, whose presence increases with the content of plant aggregates.

In addition, (Boukhattem et al., 2017) notes that for a given temperature the presence of plant fibers decreases the thermal conductivity of the composites over the whole range of water content compared to the original mortar, but that this decrease is more important in the dry state, because the insulating character of hydrophilic fibers degrades in the presence of water. The results found in this study are therefore consistent with this analysis, as C2-S and HB-S have a high content of hydrophilic plant aggregates, which explains both the low thermal conductivity in the dry state and its very marked increase in the presence of water.

We make the hypothesis that the law that describes the evolution of the thermal conductivity λ with the saturation ratio Sr takes the following form:

$$\lambda = \lambda_{dry}\,(1 + \alpha \cdot Sr) \qquad (6)$$

Where α represents a parameter which is different for each material, but which presents comparable values for materials with similar physical properties. **Figure 10** depicts the evolution of the ratio between the thermal conductivity and the dry thermal conductivity of the composites in this study and of several bio-based materials from literature with the saturation rate. It can be noted that the evolution of the thermal conductivity with saturation is approximately linear for all materials. The value of the slope of the evolution of λ/λ_{dry} with Sr has been calculated for each material and the results are presented in **Table 3**.

Table 3 Slope of the evolution of λ/λ_{dry} with Sr.

Material	$\boldsymbol{\alpha}$ **[-]**
C2-S	0.511
HB-S	0.203
C2-H+S	0.146

Sunflower pith clay composite (Brouard, 2018)	0.104
Sunflower bark pith clay composite (Brouard, 2018)	0.059
C1-H	0.089
C2-H*	0.055
Hemp composite 1 (Collet & Prétot, 2014)	0.018
Hemp composite 2 (Collet & Prétot, 2014)	0.032
Hemp composite 3 (Collet & Prétot, 2014)	0.042
Wood-based fibreboards (Troppova et al., 2014)	0.057
Basswood (Yu et al., 2011)	0.044
Larch wood (Yu et al., 2011)	0.005

These materials can be organized in separate groups, the first being hemp composites. The results of C1-H and C2-H* are compared to those of (Collet & Pretot, 2014), who studied three hemp-lime formulations with different densities ranging between 390 and 463 kg/m^3. Their dry thermal conductivity varies within a wide range, from 0.07 to 0.13 W/(m.K). We notice that the evolution of each hemp composite is different depending on the formulation and type of binder, but the slope generally increases with density.

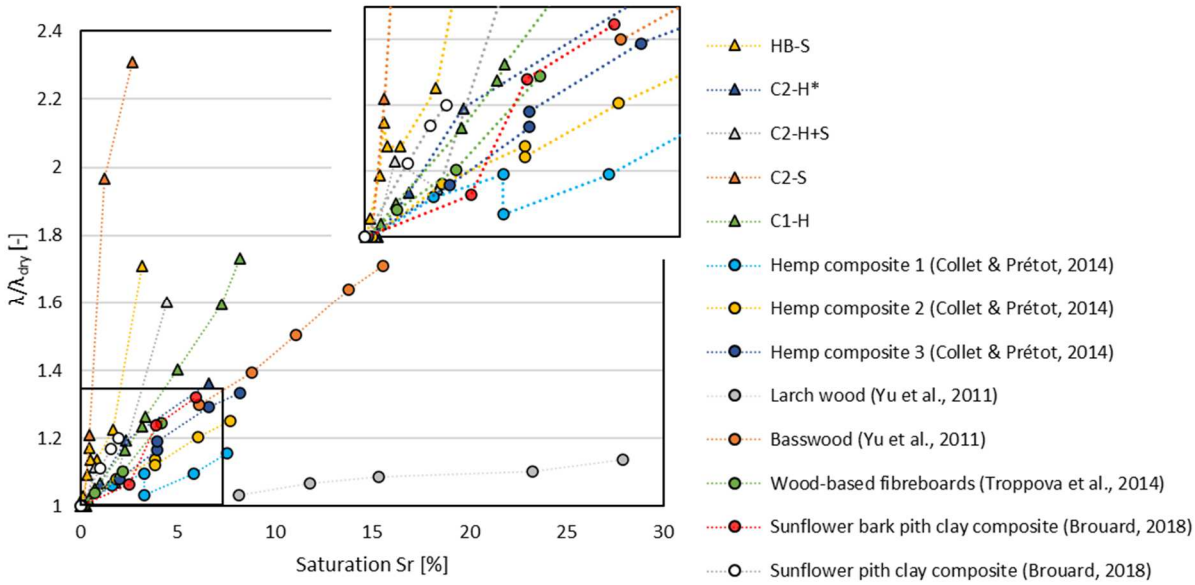

Figure 10 Evolution of thermal conductivity (normalized to the dry thermal conductivity) with saturation rate of several materials from literature and from the present study.

The second group of materials are wood and wood derivatives. (Yu et al., 2011) study larch wood and basswood, two types of wood with different $\lambda/\lambda_{dry} - Sr$ trends. Unlike the hemp aforementioned composites, these two types of wood have very different anatomies between one another. While larch wood is comprised of tracheids (narrow-lumen, short, tubular cells) oriented in the direction of the trunk and with thick walls (Liu et al., 2019), basswood presents vessels (wide-lumen, long, tubular pores) with a 50 µm diameter and thin walls, surrounded by tracheids (Gao et al., 2020).

According to (Yu et al., 2011), the difference in the structure of both woods can explain the diverse $\lambda - Sr$ trends since it causes a different distribution of the water. Furthermore, these authors studied the dry thermal conductivity of several types of wood and concluded that it increases with density ($\lambda_{dry} = 0.146$ W/(m.K) and $\rho = 672.8$ kg/m^3 for larch wood against $\lambda_{dry} = 0.073$ W/(m.K) and $\rho = 456$ kg/m^3 for basswood), which is in agreement with the results found in (Abbas et al., 2020) for bio-based materials. The last element in this group is the wood-based fiberboards studied by (Troppová et

al., 2015), which are lightweight panels (with a density of 243 kg/m^3) made up almost entirely of vegetal fibers. Thus, their thermal conductivity is very low, presenting a dry thermal conductivity of approximately 0.05 W/(m.K).

Finally, the third group of materials are sunflower composites. Two materials studied by (Brouard, 2018) are compared to HB-S, C2-S and C2-H+S, the first material being a sunflower bark-pith-clay composite with a 512 kg/m^3 density and the second, a sunflower pith-clay composite whose density is 235 kg/m^3. The dry thermal conductivity values of this group are generally lower than those of hemp composites, ranging from 0.04 to 0.09 W/(m.K). The values of HB-S and Brouard's sunflower pith composite are very close throughout the saturation range, both presenting a steep slope. In fact, all sunflower pith composites present very steep slopes, as it can be noted in **Figure 10**.

A possible explanation for this sudden increase of the thermal conductivity is that sunflower pith particles adsorb water due to their hydrophilic nature, as pith can absorb up to 917% of its weight, while hemp shiv absorbs up to 300% of its weight, according to (Magniont et al., 2012). Thus, the insulating properties of the pith particles would be considerably diminished, and with them, the insulating nature of the composite, since it is considered that the pith particles form a connected network (they represent almost half of the sample volume) through which heat is transmitted in the presence of moisture.

In conclusion, the comparison of the λ/λ_{dry} - Sr evolution of the studied composites with that of other bio-based materials from the literature shows that the structure, density, and nature of each material play a major role on its thermal response in the presence of moisture. In particular, the microstructure conditions the distribution of water within the material, the water being mainly found in the small pores (Boutin, 1996). Nevertheless, all hemp and pith composites from the present study show thermal conductivity values below 180 W/(m·K) throughout the saturation range, which stands for a good insulating performance compared to other building materials, both traditional (Breuer et al., 2020; Côté & Konrad, 2005) and bio-based (Haba et al., 2017; Khedari et al., 2001).

4.2. Impact of moisture content on thermal effusivity

The thermal effusivity has been observed to increase almost linearly with moisture content by several authors, such as (Aubert, 2013) for raw earth, (Evrard, 2008) for hemp concrete or (Houngan et al., 2015) for two kinds of wood. The evolution of some of the thermal effusivity of these materials can be observed in **Figure 11**, in which the difference $e - e_{dry}$ has been represented for clarity's sake, along with the results obtained in this experimental campaign. Although few works address the variation of the thermal effusivity of construction materials with moisture, we have chosen to only compare our results to works in which the moisture intake is a result of the ambient humidity, and not a result of a direct exposure to liquid water.

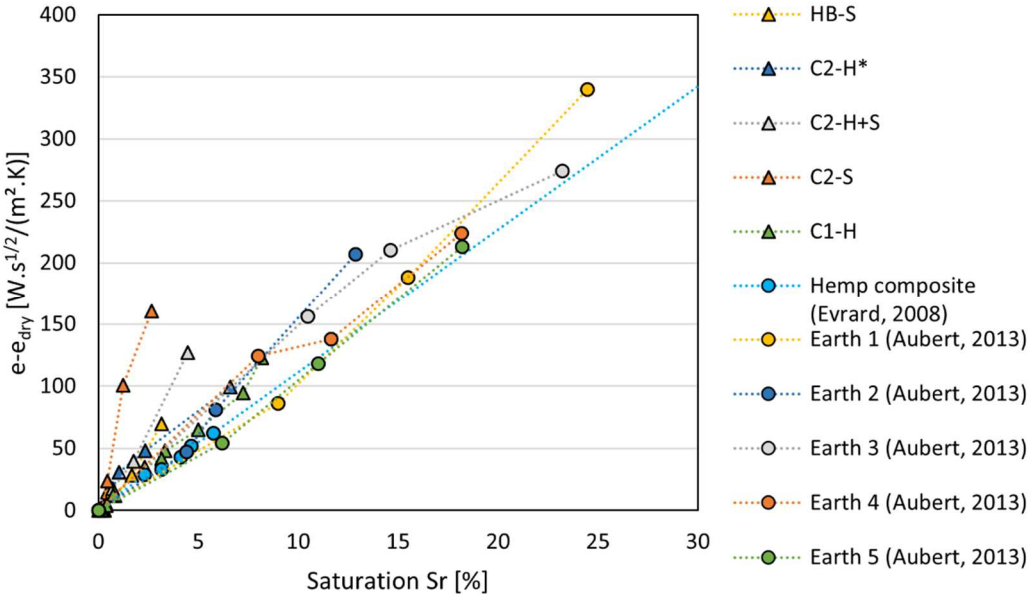

Figure 11 Evolution of the increase of thermal effusivity (in relation to the dry thermal effusivity) with saturation rate of several materials from literature and from the present study.

Aubert's raw earth samples present relatively high thermal effusivity values, between 850 and 1500 J/(m^2.K.s$^{1/2}$), while hemp and sunflower composites show values below 400 J/(m^2.K.s$^{1/2}$), but they are also more dense and less porous than the vegetal composites in the figure. C1-H is very close to Evrard's hemp concrete. Interestingly, all materials present approximately the same slope (see **Figure 11**), except for C2-S, which suggests that moisture (presented as saturation rate) has the same effect on the effusivity of most materials. In sum, all five composites from this study present a very low thermal effusivity for all relative humidity values and are therefore interesting for an indoors use. For instance, concrete has an e of 2167 J/(m^2.K.s$^{1/2}$), plaster has an e of 743 J/(m^2.K.s$^{1/2}$) and wood has an e of 399 J/(m^2.K.s$^{1/2}$), according to (Wastiels et al., 2012), whereas the highest effusivity value for the materials belonging to the present study is 359 J/(m^2.K.s$^{1/2}$).

4.3. Impact of water content on specific heat capacity

According to several studies (Allam et al., 2018; De Bruijn & Johansson, 2013; Jerman & Černý, 2012), moisture has a very important effect on the specific heat capacity of construction materials, since water's C_p is 4 to 5 times greater than the C_p of the dry material (Jerman & Černý, 2012). Unlike the effect of water on the heat transport properties, the presence of moisture in the material is beneficial in terms of heat capacity since it enhances the capacity of the material to store heat. The relation between the heat capacity of the moist material and water content in **(7)** is commonly used to predict the C_p of soils (Abu-Hamdeh, 2003; Alnefaie & Abu-Hamdeh, 2013; De Vries, 1963).

$$C_{p,wet} = \frac{\rho_{dry}}{\rho_{wet}}\left(C_{p,dry} + u \cdot C_{p,water}\right) \qquad (7)$$

Where $C_{p,dry}$ and $C_{p,wet}$ are the specific heat capacities of the dry and wet material in [J/(kg.K)], ρ_{dry} and ρ_{wet} [kg/m^3] are the dry and wet densities of the said material, u is the moisture content in kg/kg and $C_{p,water}$ is the specific heat capacity of water. The mathematical development of **(7)**, which is namely explained in (Alnefaie & Abu-Hamdeh, 2013), assumes that the thermal capacities of the gaseous phases (dry air and vapor) are negligible and that that of water and its substrate do not vary with its state of adsorption.

(Jerman & Černý, 2012) uses this expression to predict the specific heat capacity of several construction materials, but the experimental values are not provided. However, (Glass & Zelinka, 2010) study the specific heat capacity of wood and conclude that the C_p of wet material can be expressed according to **(7)** by adding an additional term that must be included to account for the energy of the bond between water and wood when the moisture content is below the fiber saturation point - a moisture threshold beyond which the physical and mechanical properties of wood substantially change (Siau, 1984).

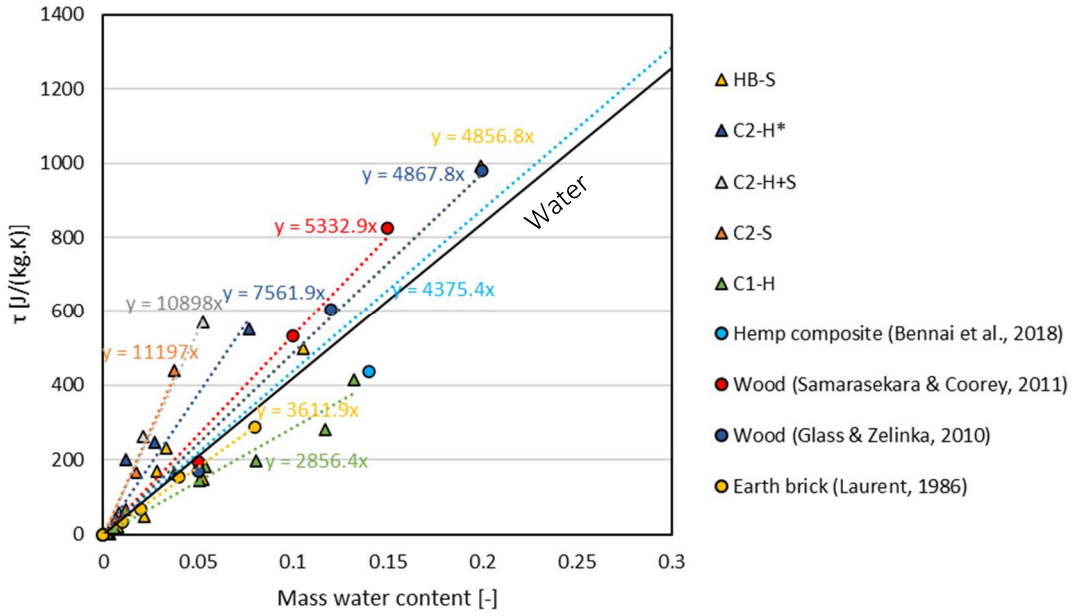

Figure 12 Evolution of specific heat capacity with the mass moisture content of several materials from literature and from the present study.

Figure 12 depicts the increase of $\tau = \frac{(\rho_{wet} \cdot C_{p,wet} - \rho_{dry} \cdot C_{p,\mathrm{dry}})}{\rho_{dry}}$ for several construction materials with mass water content, as well as the slope of the tendency for each material. According to **(7)**, the trend should be linear, and its slope should be about 4185 J/kg.K, the C_p value of liquid water. The slope of the materials in **Figure 12** shows an important variability, ranging from 2856.4 to 11197 J/kg.K. The hemp composite of Bennai et al. (Bennai et al., 2018), which was tested for water contents between 0 and 1.33 [kg/kg] by submerging the composite, shows the closest value to $C_{p,water}$, 4375.4 J/kg.K, because, for this range of water content values, free water represents a significant part of the water in the material. However, when looking at the range of water content between 0 and 0.15, which is the maximum water content found for the rest of the materials, the slope value of the hemp composite of Bennai et al. becomes 3120.4 J/kg.K. It can be noted that, generally, the lower the moisture content range for one material, the greater is the deviation of its slope from $C_{p,water}$. Some materials such as C2-S, C2-H+S, C2-H*, HB-S, the wood studied by (Samarasekara & Coorey, 2011) and the wood studied by (Glass & Zelinka, 2010) show slope values higher than $C_{p,water}$. On the other hand, C1-H and the clay brick studied by (J.-P. Laurent, 1986) show slope values lower than $C_{p,water}$.

At low water content, the water adsorbed in the material presents interactions with the material that are not negligible. These interactions can lead to additional energy, as in the case of materials with a slope greater than $C_{p,water}$. This additional energy would be an interface enthalpy related to an endothermic process. On the other hand, the behavior of materials with a slope lower than expected could be explained by the decrease in the specific heat of the adsorbed water evoked by (Mercury et

al., 2001) and (Ransom & Helgeson, 1994). Indeed, the adsorbed water would undergo a progressive phase change and acquire properties close to those of ice ($C_{p,ice}$ = 2060 J/kg.K), a state commonly denoted as “ice-like”.

Given that we can find hemp composites and pith composites with both behaviors, yet all composites with the same binder have the same tendency, it seems that the nature of the interactions between the adsorbed water and the composites mostly depends on the type of binder and not on the type of aggregate. However, it should be noted that the conductivity and effusivity tests are sensitive to measurement uncertainty and therefore these must be performed rigorously.

4.4. Water vapor permeability

Many authors have noted the influence of liquid water transport on the results of vapor permeability, such as (Antonin Fabbri, 2017), who explained that there is probably a coupling effect between water and vapor migration. Therefore, the wet and dry cup test would measure moisture transfer (liquid and vapor) and not only vapor transfer (Philip & De Vries, 1957). In other words, this test would not give direct access to δ_p but to a coefficient k_m, equal to (Ferroukhi et al., 2015):

$$k_m = \delta_p + k_l^* \qquad (8)$$

With $k_l^* = k_l \cdot \left(\frac{RT\rho_w}{M_w P_v}\right)$ a variant of the coefficient of liquid water permeability k_l that represents the hydraulic conductivity due to a partial vapor pressure gradient at constant temperature. R stands for the ideal gas constant, T stands for temperature, P_v represents the vapor pressure and ρ_w and M_w respectively represent water’s density and molar mass.

Some authors relate the increase of water vapor permeability with relative humidity to capillary condensation (Carmeliet et al., 1999; Kari et al., 1991; Pavlík et al., 2012). Specifically, (Carmeliet et al., 1999) pointed out that in hygroscopic porous and capillary materials with a wide pore size distribution, the main moisture transfer mechanisms are capillary effects and water sorption, which excludes vapor transport. They illustrated that at low relative humidity, liquid water is only present as a very thin film of adsorbed water, its thickness being only a few molecules, which is strongly bound to the pore surface and therefore does not contribute to moisture transport. At this stage, moisture transfer is governed by vapor transfer, more precisely by molecular vapor diffusion and Knudsen diffusion. As moisture saturation increases, capillary condensation occurs in the smallest pores and islands of liquid water appear, which locally increases moisture permeability, since water transfer is more efficient than vapor transfer. As saturation increases, these liquid islands proliferate and eventually converge with each other until they reach a threshold above which a connected liquid water network is established in the porous structure. At this point, a noticeable increase in moisture permeability is observed. It has also been observed that pore shape and, indirectly, hysteresis, have an impact on moisture permeability, as explained by Carmeliet et al. (Carmeliet et al., 1999).

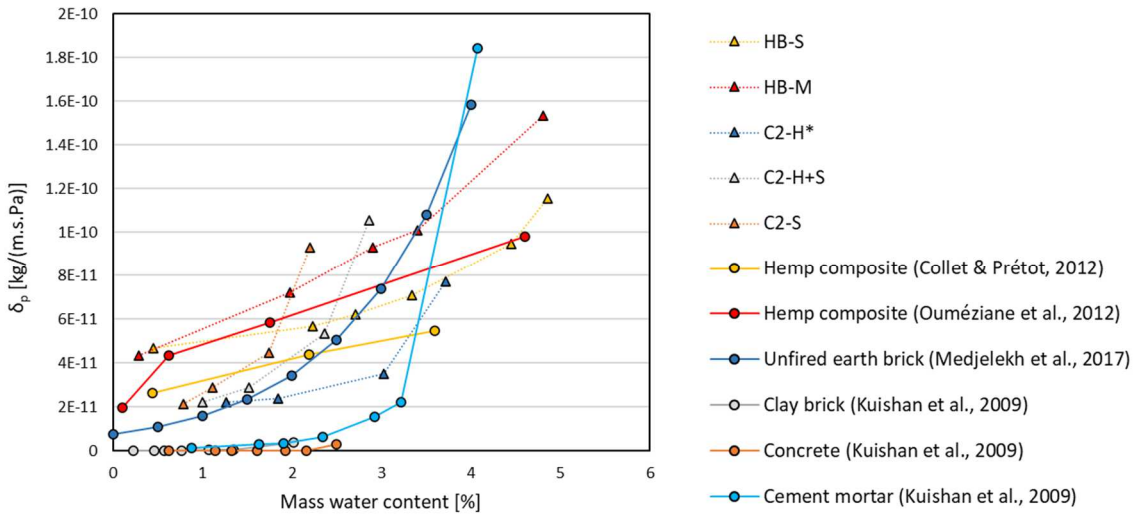

Figure 13 Evolution of the apparent water vapor permeability with mass water content of several materials from literature and the composites from this study.

Figure 13 presents a summary of the permeability results for the composites in this study, along with several construction materials listed in the literature. It represents the variation with mass water content because saturation data for the materials in the literature are not available. First, (Collet & Pretot, 2012) and (Ouméziane et al., 2012) study the variation of permeability with relative humidity and water content, respectively, of two hemp composites. Collet & Prétot's relative humidity results were transformed into water content using the adsorption isotherm provided, as the permeability tests were conducted by adsorption. The results of (Medjelekh et al., 2017) for the clay brick and the results of (Kuishan et al., 2009) for the clay brick, concrete and cement mortar are analyzed as well. Whereas the permeability of conventional concrete and clay brick by Kuishan et al. (Kuishan et al., 2009) is considerably lower, all other materials show permeability values in the same range.

For all materials, the measured permeability (which is actually the moisture permeability, as mentioned above) increases with the water content because the transport of liquid is much more efficient than that of vapor. This increase can be more or less rapid depending on the distribution of water in the material. For the materials in this study (see **Figure 9**), this distribution is conditioned by two factors: the binder and the presence of pith. Since the results for the two families of materials (C2 and HB) are quite distinct, the type of binder seems to be the main conditioner. This could be explained by the influence of pore shape on permeability mentioned by Carmeliet et al. (Carmeliet et al., 1999). Also, composites containing pith show an increase in permeability with increasing saturation. The hypothesis formulated to explain the increase in thermal conductivity of pith composites with water content is also valid for permeability: pith, which is very hydrophilic, adsorbs water even at low saturation. It is assumed that it forms connected paths, since it represents a significant part of the volume. These related pathways would serve to transport liquid water from one side of the sample to the other, significantly increasing the measured permeability. HB-S, HB-M and C2-S composites contain almost the same proportion of pith, whereas C2-H+S contains less pith and is mixed with hemp shiv particles that would interfere with the formation of connected pith pathways.

In general, all materials show an exponential increase, with the exception of the hemp composite of Collet & Prétot (Collet & Pretot, 2012) and that of Ouméziane et al. (Ouméziane et al., 2012). For the former, the growth is practically linear. For the latter, the trend describes a concave curve, contrary to the curves of the other materials, which are convex.

However, the method used in these two works is not quite the same as the method used in the present article. These authors hypothesize that the mean relative humidity in the sample corresponds to the arithmetic mean of the relative humidity inside and outside the cup. From this value, Ouméziane et al. (Ouméziane et al., 2012) uses the adsorption isotherm to indirectly determine the water content of the samples, previously dried. The same principle was applied to transform the relative humidity results of (Collet & Pretot, 2012) into water content. To evaluate the pertinence of this method, the experimental water content is compared in **Figure 14** with those corresponding respectively to the adsorption isotherm, the desorption isotherm and the average sorption-desorption for the C2-H*, C2-H+S, C2-S, HB-S and HB-M formulations.

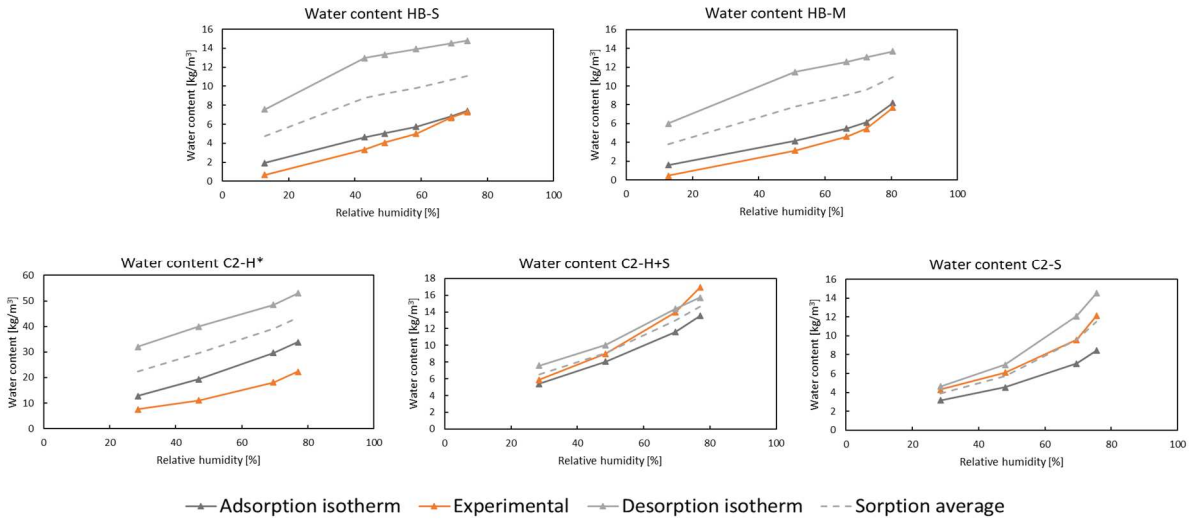

Figure 14 Comparison between experimental water content and the water content corresponding to the relative humidity (calculated as the mean value of the relative humidity pair) for each permeability test according to the adsorption isotherm, the desorption isotherm, and the mean value of both.

The results in **Figure 14** are divergent. Whilst the experimental water content is close to the mean between adsorption and desorption for C2-H+S and C2-S, it is close to the adsorption curve for HB-S and HB-M. However, in the case of C2-H*, the experimental determination yields values significantly lower than the adsorption curve. Consequently, the method used by Collet & Prétot and by Ouméziane et al. (Ouméziane et al., 2012) cannot be applied in a generalized way for the materials of this experimental campaign.

A second approach is to average the relative humidity at the upper and lower surface of the sample, which can be calculated using the β-correction, following **(3)** and **(4)**. These values should be more accurate because they are supposed to reflect the true moisture conditions at the sample boundary. **Figure 15** shows the water content corresponding to the adsorption and desorption curve, as well as the water content corresponding to the average of the two, for the mean value of the upper and lower surface humidity.

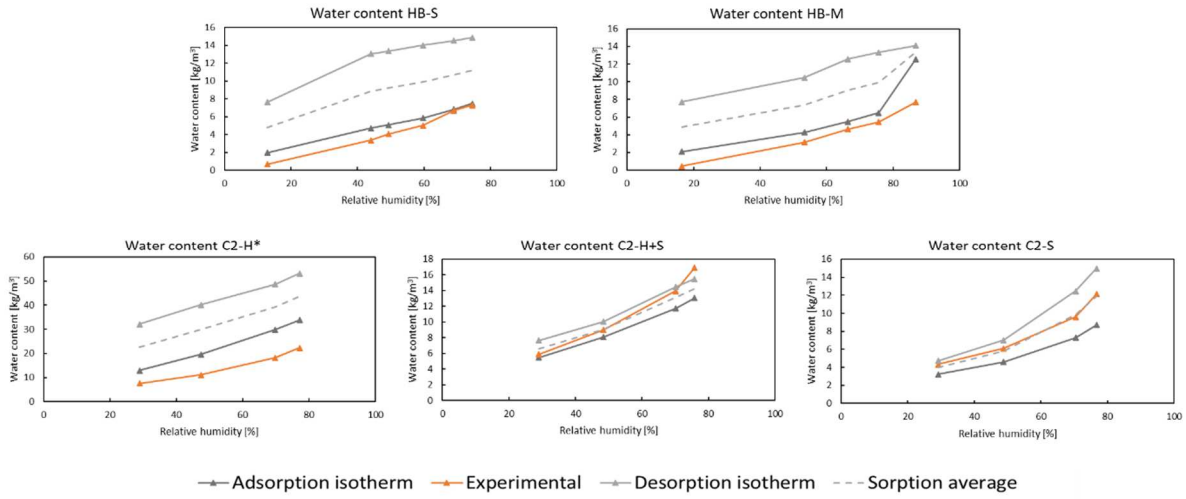

Figure 15 Comparison between experimental water content and the water content corresponding to the relative humidity (calculated as the mean value between the upper and lower surface relative humidity) for each permeability test according to the adsorption isotherm, the desorption isotherm, and the mean value of both.

The differences with **Figure 14** are barely noticeable, as the average relative humidity at the surface is very close to the average relative humidity in the surrounding air. Therefore, this approach, like the previous one, cannot be applied in a generalized manner.

Both methods assume that the vapor pressure follows a linear variation along the thickness of the sample, with maximum and minimum values corresponding to the vapor pressure values imposed on the inside and outside of the wet cup, or conversely for the dry cup (or P_v at the surface calculated using the β-correction). With this assumption, the mean value of the water content, which is a function of the vapor pressure, can be calculated as the water content corresponding to the arithmetic mean of the relative humidity values at the limits. To evaluate the validity of this assumption, at the end of the permeability test, a 6 cm thick sample of each formulation was perforated 3 times on the same vertical half-plane, as shown in **Figure 16**, to measure the relative humidity at the center of the sample at several heights using a ROTRONIC humidity and temperature sensor. Position A is 1.5 cm from the upper surface, position B is 3 cm from the upper surface and position C is 1.5 cm from the lower surface. The sensor is inserted in positions A, B and C, one at a time.

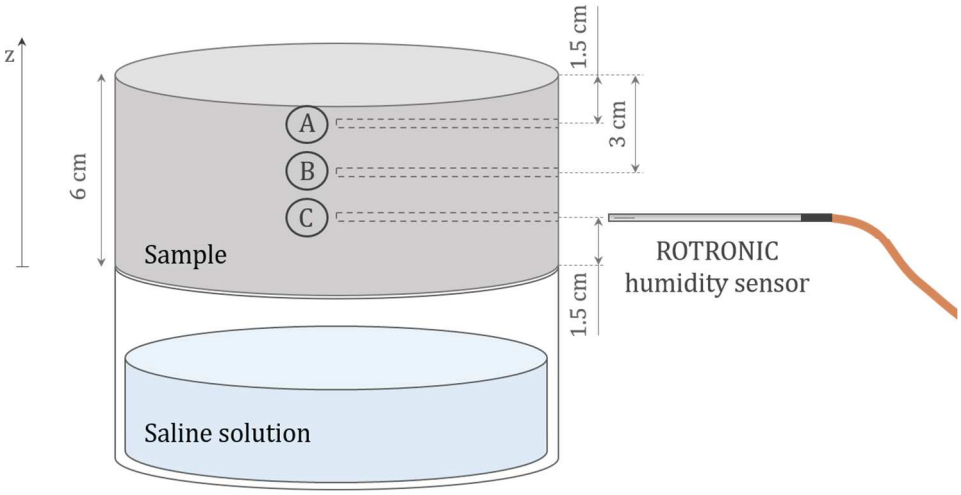

Figure 16 Illustration of the measuring device of relative humidity's vertical variation.

The results of the latter test are shown in **Figure 17**. The moisture value at z = 0 cm corresponds to the moisture value at the lower surface calculated using the β-correction, the value at z = 1.5 cm corresponds to position C, the value at z = 3 cm corresponds to position B, z = 4.5 cm corresponds to position A and, finally, z = 6 cm corresponds to the moisture value at the upper surface calculated using the β-correction. For each formulation, only one humidity pair was selected, with the exception of HB-S, for which one dry and one wet cup were tested.

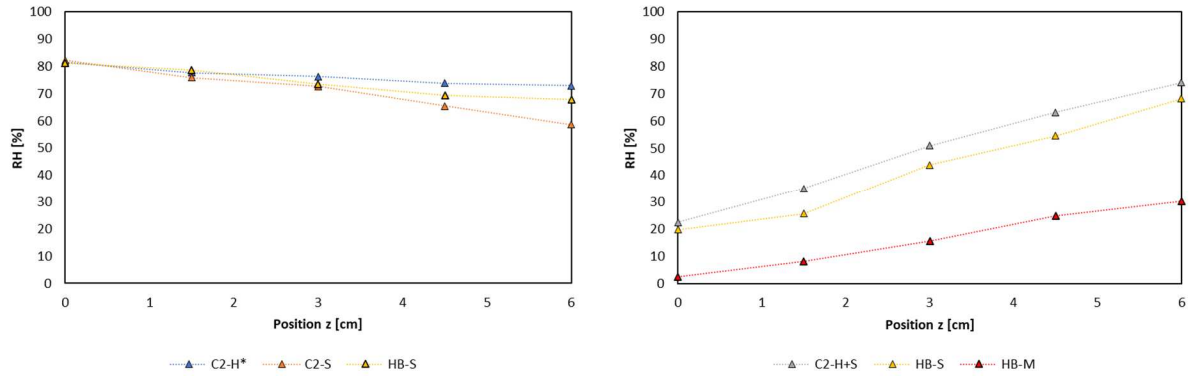

Figure 17 Variation of relative humidity with the position following the vertical axis of several wet cups (left) and several dry cups (right).

For all samples tested, the variation in moisture content with thickness is practically linear, which validates the hypothesis that allows us to calculate the average moisture content of the sample through the arithmetic mean of the relative humidity at the limits. Based on the results in **Figure 15**, the choice of averaging the surface moistures is more appropriate than averaging the moistures inside and outside the cup. Although the moisture varies linearly along the vertical axis, heterogeneity in the radial distribution of moisture was noted, with the center of the sample being wetter than the edges.

Therefore, the experimental moisture content should lie between the adsorption isotherm and the desorption isotherm of each material. The discrepancy found for some materials in **Figure 13** may be due to the ageing of the materials, since it has been observed that sorption isotherms evolve after several adsorption-desorption cycles (Chennouf et al., 2018).

5. Conclusion

In this article, the variation of transport and storage hygrothermal properties with moisture content was analyzed for composites made from maize pith, sunflower pith, and hemp shiv. This information is used to enrich existing databases and to feed the hygrothermal transfer models in order to improve their prediction. Indeed, models often neglect the influence of humidity on material properties. In most cases, tests have shown a material response very similar to that of materials in the literature, however, sunflower pith composites have shown a particular sensitivity to moisture with respect to thermal conductivity and apparent vapor permeability. The main findings of this study are summarized below:

- Thermal conductivity and thermal effusivity present a proportional evolution with the variation of the degree of saturation, which depends on the hygrometric environment of the material. However, the impact of humidity on these thermal properties of the studied bio-based materials varies from one composite to another depending on the binder type and the plant aggregate's nature.
- Concerning the specific heat capacity, a linear variation with the water content is observed for the studied biobased composites, which is in accordance with the literature. However, for low

water contents (hygroscopic conditions), the commonly used mixing law for the estimation of the specific heat is not always verified for this kind of building materials and a direct experimental assessment of this parameter seems necessary.

- The water vapor permeability evolves exponentially with the water content for most bio-based materials. The type of binder, the nature and the quantity of the vegetal aggregates represent the main parameters which impact the variation of this moisture transfer property.
- It has been shown as well that the transport of liquid water, called k_l^*, has a significant role in the hygroscopic transfers that take place within the material and should therefore be considered in numerical models.
- In wet and dry cup tests, we recommend to measure the moisture content by evaluating the sample's mass gain rather than using the adsorption or desorption isotherms (or their average) since none of them correctly describe the experimental results obtained in this campaign.

Acknowledgments

This work has been supported by the French environmental and energy management agency (ADEME).

References

Abbas, M. S., Fabbri, A., Ferroukhi, M. Y., Gourdon, E., & Mcgregor, F. (2021). Link between acoustic and hygrothermal behavior of hemp shiv and pith composites. *4th International Conference on Bio-Based Building Materials*, 1–9.

Abbas, M. S., Gourdon, E., Glé, P., McGregor, F., Ferroukhi, M. Y., & Fabbri, A. (2021). Relationship between hygrothermal and acoustical behavior of hemp and sunflower composites. *Building and Environment*, *188*(October 2020). https://doi.org/10.1016/j.buildenv.2020.107462

Abbas, M. S., Mcgregor, F., Fabbri, A., & Ferroukhi, M. Y. (2020). The use of pith in the formulation of lightweight bio-based composites : impact on mechanical and hygrothermal properties. *Construction and Building Materials*, *259*. https://doi.org/10.1016/j.conbuildmat.2020.120573

Abbas, M. S., McGregor, F., Fabbri, A., & Ferroukhi, Y. (2019). Influence of origin and year of harvest on the performance of pith mortars. *3rd International Conference of Bio-Based Building Materials*, 42–48.

Abu-Hamdeh, N. H. (2003). Thermal properties of soils as affected by density and water content. *Biosystems Engineering*, *86*(1), 97–102. https://doi.org/10.1016/S1537-5110(03)00112-0

Al-Homoud, M. S. (2005). Performance characteristics and practical applications of common building thermal insulation materials. *Building and Environment*, *40*(3), 353–366. https://doi.org/10.1016/j.buildenv.2004.05.013

Allam, R., Issaadi, N., Belarbi, R., El-Meligy, M., & Altahrany, A. (2018). Hygrothermal behavior for a clay brick wall. *Heat and Mass Transfer/Waerme- Und Stoffuebertragung*, *54*(6), 1579–1591. https://doi.org/10.1007/s00231-017-2271-5

Allinson, D., & Hall, M. (2010). Hygrothermal analysis of a stabilised rammed earth test building in the UK. *Energy and Buildings*, *42*(6), 845–852. https://doi.org/10.1016/j.enbuild.2009.12.005

Alnefaie, K. A., & Abu-Hamdeh, N. H. (2013). Specific heat and volumetric heat capacity of granular materials as affected by moisture and density. *Applied Mechanics and MaterialsProceedings of the 2013 International Conference on Mechanics, Fluids, Heat, Elasticity and Electromagnetic Fields*, 139–143. https://doi.org/10.4028/www.scientific.net/AMM.575.103

Amziane, S., Collet, F., Lawrence, M., Magniont, C., Picandet, V., & Sonebi, M. (2017). Recommendation of the RILEM TC 236-BBM: characterisation testing of hemp shiv to determine

the initial water content, water absorption, dry density, particle size distribution and thermal conductivity. *Materials and Structures/Materiaux et Constructions*, *50*(3). https://doi.org/10.1617/s11527-017-1029-3

Amziane, S., & Sonebi, M. (2016). Overview on biobased building material made with plant aggregate. In *RILEM Technical Letters* (Vols. 2016-Augus, Issue June). https://doi.org/10.21809/rilemtechlett.v1.9

Antczak, E., Chauchois, A., Defer, D., & Duthoit, B. (2003). Characterisation of the thermal effusivity of a partially saturated soil by the inverse method in the frequency domain. *Applied Thermal Engineering*, *23*(12), 1525–1536. https://doi.org/10.1016/S1359-4311(03)00084-X

Arvalis. (2020). *MAÏS GRAIN : RETOUR SUR LES FAITS MARQUANTS DE LA CAMPAGNE 2020*. https://www.arvalis-infos.fr/ma-s-grain-un-rendement-national-proche-de-90-q/ha-@/view-33708-arvarticle.html

Association construire en chanvre, & Fédération Française du Bâtiment. (2009). *Construire en chanvre -Règles professionelles d'exécution* (SEBTP (ed.); 2ème éditi). Fédération Française du Bâtiment.

Aubert, J.-E. (2013). Caractérisation des briques de terre crue de Midi-Pyrénées. In *Rapport final du projet TERCRUSO*.

Belkharchouche, D., & Chaker, A. (2016). Effects of moisture on thermal conductivity of the lightened construction material. *International Journal of Hydrogen Energy*, *41*(17), 7119–7125. https://doi.org/10.1016/j.ijhydene.2016.01.160

Bennai, F., Issaadi, N., Abahri, K., Belarbi, R., & Tahakourt, A. (2018). Experimental characterization of thermal and hygric properties of hemp concrete with consideration of the material age evolution. *Heat and Mass Transfer/Waerme- Und Stoffuebertragung*, *54*(4), 1189–1197. https://doi.org/10.1007/s00231-017-2221-2

Bouguerra, A. (1999). Temperature and moisture dependence on the thermal conductivity of wood-cement-based composite: experimental and theoretical analysis. *Journal of Physics D: Applied Physics*, *32*(21), 2797–2803. https://doi.org/10.1088/0022-3727/32/21/313

Bouguerra, A., Diop, M. B., Laurent, J. P., Benmalek, M. L., & Queneudec, M. (1998). Effect of moisture content on the thermal effusivity of wood cement-based composites. *Journal of Physics D: Applied Physics*, *31*(24), 3457–3462. https://doi.org/10.1088/0022-3727/31/24/008

Bouguerra, A., Ledhem, A., Laurent, J. P., Diop, M. B., & Queneudec, M. (1998). Thermal effusivity of two-phase wood cement-based composites. *Journal of Physics D: Applied Physics*, *31*(17), 2184–2190. https://doi.org/10.1088/0022-3727/31/17/017

Boukhattem, L., Boumhaout, M., Hamdi, H., Benhamou, B., & Ait Nouh, F. (2017). Moisture content influence on the thermal conductivity of insulating building materials made from date palm fibers mesh. *Construction and Building Materials*, *148*, 811–823. https://doi.org/10.1016/j.conbuildmat.2017.05.020

Boutin, C. (1996). Conductivité thermique du béton cellulaire autoclavé: Modélisation par méthode autocohérente. *Materials and Structures/Materiaux et Constructions*, *29*(194), 609–615.

Breuer, S., Schwotzer, M., Speziale, S., & Schilling, F. R. (2020). Thermoelastic properties of synthetic single crystal portlandite Ca(OH)2 - Temperature-dependent thermal diffusivity with derived thermal conductivity and elastic constants at ambient conditions. *Cement and Concrete Research*, *137*(August). https://doi.org/10.1016/j.cemconres.2020.106199

Brouard, Y. (2018). *Caractérisation et optimisation d'un composite biosourcé pour l'habitat*. http://theses.insa-lyon.fr/publication/2005isal0037/these.pdf

Brouard, Y., Belayachi, N., Hoxha, D., Méo, S., & Abdallah, W. (2017). Hygrothermal Behavior of Clay - Sunflower (*Helianthus annuus*) and Rape Straw (*Brassica napus*) Plaster Bio-Composites for Building Insulation. *Advanced Engineering Forum*, *21*, 242–248. https://doi.org/10.4028/www.scientific.net/aef.21.242

Brouard, Y., Belayachi, N., Hoxha, D., Ranganathan, N., & Méo, S. (2018). Mechanical and hygrothermal behavior of clay – Sunflower (Helianthus annuus) and rape straw (Brassica napus) plaster bio-composites for building insulation. *Construction and Building Materials*, *161*, 196–207. https://doi.org/10.1016/j.conbuildmat.2017.11.140

Cagnon, H., Aubert, J. E., Coutand, M., & Magniont, C. (2014). Hygrothermal properties of earth bricks. *Energy & Buildings*, *80*, 208–217. https://doi.org/10.1016/j.enbuild.2014.05.024

Carmeliet, J., Descamps, F., & Houvenaghel, G. (1999). A multiscale network model for simulating moisture transfer properties of porous media. *Transport in Porous Media*, *35*(1), 67–88. https://doi.org/10.1023/A:1006500716417

Chennouf, N., Agoudjil, B., Boudenne, A., Benzarti, K., & Bouras, F. (2018). Hygrothermal characterization of a new bio-based construction material: Concrete reinforced with date palm fibers. *Construction and Building Materials*, *192*, 348–356. https://doi.org/10.1016/j.conbuildmat.2018.10.089

Cholewa, T., Balaras, C. A., Nižetić, S., & Siuta-Olcha, A. (2020). On calculated and actual energy savings from thermal building renovations – Long term field evaluation of multifamily buildings. *Energy and Buildings*, *223*. https://doi.org/10.1016/j.enbuild.2020.110145

Colinart, T., Glouannec, P., Pierre, T., & Chauvelon, P. (2013). Hygrothermal behaviour of a hemp concrete wall: Comparison between experimental and numerical results. *Proceedings of BS 2013: 13th Conference of the International Building Performance Simulation Association*, 2852–2859.

Collet, F., & Pretot, S. (2012). Experimental investigation of moisture buffering capacity of sprayed hemp concrete. *Construction and Building Materials*, *36*, 58–65. https://doi.org/10.1016/j.conbuildmat.2012.04.139

Collet, F., & Pretot, S. (2014). Thermal conductivity of hemp concretes: Variation with formulation, density and water content. *Construction and Building Materials*, *65*, 612–619. https://doi.org/10.1016/j.conbuildmat.2014.05.039

Côté, J., & Konrad, J.-M. (2005). A generalized thermal conductivity model for soils and construction materials. *Canadian Geotechnical Journal*, *42*(2), 443–458. https://doi.org/10.1139/t04-106

De Bruijn, P., & Johansson, P. (2013). Moisture fixation and thermal properties of lime-hemp concrete. *Construction and Building Materials*, *47*, 1235–1242. https://doi.org/10.1016/j.conbuildmat.2013.06.006

De Vries, D. A. (1963). Thermal properties of soils. In W. R. van Wijk (Ed.), *Physics of plant environment* (pp. 210–235). John Wiley & Sons.

Evrard, A. (2008). *Transient hygrothermal behavior of Lime-Hemp Materials*. UNIVERSITE CATHOLIQUE DE LOUVAIN Ecole Polytechnique de Louvain.

Fabbri, A., & McGregor, F. (2017). Impact of the determination of the sorption-desorption curves on the prediction of the hemp concrete hygrothermal behaviour. *Construction and Building*

Materials, *157*, 108–116. https://doi.org/10.1016/j.conbuildmat.2017.09.077

Fabbri, Antonin. (2017). *Habilitation à diriger les recherches : Physics and Mechanics of porous media for civil engineering applications*.

Ferroukhi, M. Y., Abahri, K., Belarbi, R., Limam, K., & Nouviaire, A. (2015). Experimental validation of coupled heat , air and moisture transfer modeling in multilayer building components. *Heat and Mass Transfer*, *December*. https://doi.org/10.1007/s00231-015-1740-y

Gao, H., Yang, M., Dang, B., Luo, X., Liu, S., Li, S., Chen, Z., & Li, J. (2020). Natural phenolic compound-iron complexes: Sustainable solar absorbers for wood-based solar steam generation devices. *RSC Advances*, *10*(2), 1152–1158. https://doi.org/10.1039/c9ra08235b

Glass, S. V, & Zelinka, S. L. (2010). Moisture Relations and Physical Properties of Wood. In *Wood handbook: wood as an engineering material* (Centennial, pp. 4-1-4–19). U.S. Dept. of Agriculture, Forest Service, Forest Products Laboratory.

Gourlay, E., Glé, P., Marceau, S., Foy, C., & Moscardelli, S. (2017). Effect of water content on the acoustical and thermal properties of hemp concretes. *Construction and Building Materials*, *139*, 513–523. https://doi.org/10.1016/j.conbuildmat.2016.11.018

Grillone, B., Danov, S., Sumper, A., Cipriano, J., & Mor, G. (2020). A review of deterministic and data-driven methods to quantify energy efficiency savings and to predict retrofitting scenarios in buildings. *Renewable and Sustainable Energy Reviews*, *131*(March), 110027. https://doi.org/10.1016/j.rser.2020.110027

Guyomard, S. (2020). *Les cultures de printemps à l'honneur*. Terre-Net. https://www.terre-net.fr/observatoire-technique-culturale/strategie-technique-culturale/article/les-cultures-de-printemps-a-l-honneur-en-2020-217-169059.html

Haba, B., Agoudjil, B., Boudenne, A., & Benzarti, K. (2017). Hygric properties and thermal conductivity of a new insulation material for building based on date palm concrete. *Construction and Building Materials*, *154*, 963–971. https://doi.org/10.1016/j.conbuildmat.2017.08.025

Hall, M., & Allinson, D. (2009). Assessing the effects of soil grading on the moisture content-dependent thermal conductivity of stabilised rammed earth materials. *Applied Thermal Engineering*, *29*(4), 740–747. https://doi.org/10.1016/j.applthermaleng.2008.03.051

Houngan, C. A., Awanto, C., Djossou, A. A., Anjorin, M., & Vianou, A. (2015). Measurement of Thermal Effusivity and Thermal Conductivityat Various Water Content for Two Tropical Wood Species. *Procedia Engineering*, *127*, 48–55. https://doi.org/10.1016/j.proeng.2015.11.328

Howlader, M. K., Rashid, M. H., Mallick, D., & Haque, T. (2012). Effects of aggregate types on thermal properties of concrete. *ARPN Journal of Engineering and Applied Sciences*, *7*(7), 900–907.

InterChanvre. (2018). *Le chanvre. La culture écologique, agronomique et éco-responsable*.

International Energy Agency, & UN Environment Programme. (2019). *2019 Global Status Report for Buildings and Construction: Towards a zero-emission, efficient and resilient buildings and construction sector*. Global Alliance for Buildings and Construction.

International Energy Agency, & UN Environment Programme. (2020). *2020 Global Status Report for Buildings and Construction*.

International Organization for Standardization. (2007). *ISO 8894-2:2007, Refractory materials - Determination of thermal conductivity - Part 2: Hot-wire method (parallel)*.

International Organization for Standardization. (2016). *NF EN ISO 12572:2016, Hygrothermal*

performance of building materials and products - Determination of water vapour transmission properties - Cup method.

Jerman, M., & Černý, R. (2012). Effect of moisture content on heat and moisture transport and storage properties of thermal insulation materials. *Energy and Buildings*, *53*, 39–46. https://doi.org/10.1016/j.enbuild.2012.07.002

Kari, B., Perrin, B., & Foures, J. C. (1991). Perméabilité h la vapeur d'eau de matériaux de construction: calcul numérique. *Materials and Structures*, *24*, 227–233.

Khedari, J., Suttisonk, B., Pratinthong, N., & Hirunlabh, J. (2001). New lightweight composite construction materials with low thermal conductivity. *Cement and Concrete Composites*, *23*(1), 65–70. https://doi.org/10.1016/S0958-9465(00)00072-X

Kočí, V., Vejmelková, E., Čáchová, M., Koňáková, D., Keppert, M., Maděra, J., & Černý, R. (2017). Effect of Moisture Content on Thermal Properties of Porous Building Materials. *International Journal of Thermophysics*, *38*(2). https://doi.org/10.1007/s10765-016-2164-8

Kuishan, L., Xu, Z., & Jun, G. (2009). Experimental investigation of hygrothermal parameters of building materials under isothermal conditions. *Journal of Building Physics*, *32*(4), 355–370. https://doi.org/10.1177/1744259108102832

Latif, E., Tucker, S., Ciupala, M. A., Wijeyesekera, D. C., & Newport, D. (2014). Hygric properties of hemp bio-insulations with differing compositions. *Construction and Building Materials*, *66*, 702–711. https://doi.org/10.1016/j.conbuildmat.2014.06.021

Laurent, J.-P. (1986). *Contribution à la caractérisation thermique des milieux poreux granulaires* (Issue January 1986). Institut National Polytechnique de Grenoble.

Laurent, J. P., & Guerre-Chaley, C. (1995). Influence de la teneur en eau et de la température sur la conductivité thermique du béton cellulaire autoclavé. *Materials and Structures*, *28*(8), 464–472. https://doi.org/10.1007/BF02473166

Lei, H., Fu, C., Zou, Y., Guo, S., & Huo, J. (2019). Thermal energy storage composite with sensing function and its thermal conductivity and thermal effusivity enhancement. *Journal of Materials Chemistry A*, *7*(12), 6720–6729. https://doi.org/10.1039/c8ta11753e

Liu, M., Li, C., & Wang, Q. (2019). Microstructural characteristics of larch wood treated by high-intensity microwave. *BioResources*, *14*(1), 1174–1184. https://doi.org/10.15376/biores.14.1.1174-1184

Liuzzi, S., Rubino, C., Stefanizzi, P., Petrella, A., Boghetich, A., Casavola, C., & Pappalettera, G. (2018). Hygrothermal properties of clayey plasters with olive fibers. *Construction and Building Materials*, *158*, 24–32. https://doi.org/10.1016/j.conbuildmat.2017.10.013

Lu, D. B., & Warsinger, D. M. (2020). Energy savings of retrofitting residential buildings with variable air volume systems across different climates. *Journal of Building Engineering*, *30*(June 2019), 101223. https://doi.org/10.1016/j.jobe.2020.101223

Magniont, C., Escadeillas, G., Coutand, M., & Oms-Multon, C. (2012). Use of plant aggregates in building ecomaterials. *European Journal of Environmental and Civil Engineering*, *16*(SUPPL. 1). https://doi.org/10.1080/19648189.2012.682452

McGregor, F., Fabbri, A., Ferreira, J., Simões, T., Faria, P., & Morel, J. C. (2017). Procedure to determine the impact of the surface film resistance on the hygric properties of composite clay/fibre plasters. *Materials and Structures/Materiaux et Constructions*, *50*(4). https://doi.org/10.1617/s11527-017-1061-3

McGregor, F., Heath, A., Fodde, E., & Shea, A. (2014). Conditions affecting the moisture buffering measurement performed on compressed earth blocks. *Building and Environment*, *75*, 11–18. https://doi.org/10.1016/j.buildenv.2014.01.009

Medjelekh, D., Ulmet, L., & Dubois, F. (2017). Characterization of hygrothermal transfers in the unfired earth. *Energy Procedia*, *139*, 487–492. https://doi.org/10.1016/j.egypro.2017.11.242

Mercury, L., Vieillard, P., & Tardy, Y. (2001). Thermodynamics of ice polymorphs and "ice-like" water in hydrates and hydroxides. *Applied Geochemistry*, *16*(2), 161–181. https://doi.org/10.1016/S0883-2927(00)00025-1

Meukam, P., Jannot, Y., Noumowe, A., & Kofane, T. C. (2004). Thermo physical characteristics of economical building materials. *Construction and Building Materials*, *18*(6), 437–443. https://doi.org/10.1016/j.conbuildmat.2004.03.010

Ouméziane, Y. A., Moissette, S., Bart, M., & Lanos, C. (2012). Effect of coating on the hygric performance of a hemp concrete wall To cite this version : Effect of coating on the hygric performance of a hemp concrete wall. *5th IBPC*, 109–116. https://hal.archives-ouvertes.fr/hal-00801140

Palumbo, M., McGregor, F., Heath, A., & Walker, P. (2016). The influence of two crop by-products on the hygrothermal properties of earth plasters. *Building and Environment*, *105*, 245–252. https://doi.org/10.1016/j.buildenv.2016.06.004

Pavlík, Z., Žumár, J., Pavlíková, M., & Černý, R. (2012). A Boltzmann transformation method for investigation of water vapor transport in building materials. *Journal of Building Physics*, *35*(3), 213–223. https://doi.org/10.1177/1744259111418329

Pennec, F., Alzina, A., Tessier-Doyen, N., Naït-Ali, B., Mati-Baouche, N., De Baynast, H., & Smith, D. S. (2013). A combined finite-discrete element method for calculating the effective thermal conductivity of bio-aggregates based materials. *International Journal of Heat and Mass Transfer*, *60*(1), 274–283. https://doi.org/10.1016/j.ijheatmasstransfer.2013.01.002

Philip, J. R., & De Vries, D. A. (1957). Moisture movement in porous materials under temperature gradients. *Transactions, American Geophysical Union*, *38*(2), 222–232. https://doi.org/10.1029/TR038i002p00222

Rahim, M., Douzane, O., Tran Le, A. D., Promis, G., & Langlet, T. (2016). Characterization and comparison of hygric properties of rape straw concrete and hemp concrete. *Construction and Building Materials*, *102*, 679–687. https://doi.org/10.1016/j.conbuildmat.2015.11.021

Ransom, B., & Helgeson, H. C. (1994). Estimation of the standard molal heat capacities, entropies and volumes of 2:1 clay minerals. *Geochimica et Cosmochimica Acta*, *58*(21), 4537–4547. https://doi.org/10.1016/0016-7037(94)90189-9

Real, S., Bogas, J. A., Glória, G. M., & Ferrer, B. (2016). Thermal conductivity of structural lightweight aggregate concrete. *Magazine of Concrete Research*, *68*(15), 798–808. https://doi.org/10.1680/jmacr.15.00424

Sadineni, S. B., Madala, S., & Boehm, R. F. (2011). Passive building energy savings: A review of building envelope components. *Renewable and Sustainable Energy Reviews*, *15*(8), 3617–3631. https://doi.org/10.1016/j.rser.2011.07.014

Samarasekara, S. A. L., & Coorey, R. V. (2011). Thermal capacity as a function of moisture content of Sri Lankan wood species: Wheatstone bridge method. *Proceedings of the 27th Technical Sessions - Institute of Physics*, *27*(January), 9–16.

Seng, B., Magniont, C., Spagnol, S., & Lorente, S. (2017). Assessment of a precast hemp concrete hygrothermal properties. *2nd International Conference on Bio-Based Building Materials & 1st Conference on ECOlogical Valorisation of GRAnular and FIbrous Materials*, *35*(2), 386–393.

Shrotriya, A. K., Verma, L. S., Singh, R., & Chaudhary, D. R. (1991). Prediction of heat storage coefficient of some loose granular materials on the basis of structure and packing of the grains. *Heat Recovery Systems and CHP*, *11*(5), 423–430. https://doi.org/10.1016/0890-4332(91)90010-2

Siau, J. F. (1984). *Transport processes in wood*. Springer.

Taoukil, D., El Bouardi, A., Sick, F., Mimet, A., Ezbakhe, H., & Ajzoul, T. (2013). Moisture content influence on the thermal conductivity and diffusivity of wood-concrete composite. *Construction and Building Materials*, *48*, 104–115. https://doi.org/10.1016/j.conbuildmat.2013.06.067

Toman, J., & Černý, R. (2001). Temperature and Moisture Dependence of the Specific Heat of High Performance Concrete. *Acta Polytechnica*, *41*(1), 6–8. https://doi.org/10.14311/172

Tran Le, A. D. (2010). *Etude des transferts hygrothermiques dans le béton de chanvre et leur application au bâtiment*. Université de Reims - Champagne Ardenne.

Troppová, E., Švehlík, M., Tippner, J., & Wimmer, R. (2015). Influence of temperature and moisture content on the thermal conductivity of wood-based fibreboards. *Materials and Structures/Materiaux et Constructions*, *48*(12), 4077–4083. https://doi.org/10.1617/s11527-014-0467-4

Vololonirina, O., Coutand, M., & Perrin, B. (2014). Characterization of hygrothermal properties of wood-based products - Impact of moisture content and temperature. *Construction and Building Materials*, *63*, 223–233. https://doi.org/10.1016/j.conbuildmat.2014.04.014

Walker, R., & Pavía, S. (2014). Moisture NON transfer and thermal properties of hemp – lime concretes. *Construction and Building Materials*, *64*, 270–276. https://doi.org/10.1016/j.conbuildmat.2014.04.081

Wastiels, L., Schifferstein, H. N. J., Heylighen, A., & Wouters, I. (2012). Relating material experience to technical parameters: A case study on visual and tactile warmth perception of indoor wall materials. *Building and Environment*, *49*(1), 359–367. https://doi.org/10.1016/j.buildenv.2011.08.009

Yu, Z. T., Xu, X., Fan, L. W., Hu, Y. C., & Cen, K. F. (2011). Experimental measurements of thermal conductivity of wood species in China: Effects of density, temperature, and moisture content. *Forest Products Journal*, *61*(2), 130–135. https://doi.org/10.13073/0015-7473-61.2.130